Building blocks of amorphous $Ge_2Sb_2Te_5$

Christian Lang,[1] Se Ahn Song,[2] Duc Nguyen Manh,[3] and David J. H. Cockayne[1]
[1]*Department of Materials, University of Oxford, Parks Road, Oxford OX1 3PH, United Kingdom*
[2]*Analytical Engineering Center, Samsung Advanced Institute of Technology, Yongin 446-712, Korea*
[3]*EURATOM/UKAEA Fusion Association, Culham Science Centre, Abingdon OX14 3DB, United Kingdom*
(Received 14 March 2007; published 1 August 2007)

The structural changes during the phase change between the amorphous and crystalline phase in $Ge_2Sb_2Te_5$ have been the subject of intense study due to the importance of $Ge_2Sb_2Te_5$ in phase change memory devices. In our study, the energetics of the transition between the crystalline and the amorphous phase of $Ge_2Sb_2Te_5$ is explored using density functional theory (DFT) calculations, electron diffraction, and reverse Monte Carlo model refinement. No energy barrier was found between the crystalline and the previously suggested amorphous structure of $Ge_2Sb_2Te_5$. Further DFT calculations have led to a different building block of the amorphous structure, which is shown to agree with the experimental reduced density function determined from electron diffraction experiments and previously reported extended x-ray absorption fine structure measurements.

DOI: 10.1103/PhysRevB.76.054101 PACS number(s): 61.43.Dq, 61.14.−x

I. INTRODUCTION

Rapid phase change materials, and particularly the GeSbTe alloy system, are attracting considerable interest because of their possible use in the active layer of high density storage devices such as the digital versatility disk and phase change random access memory test devices.[1,2] In these devices, information is encoded by creating amorphous spots in a polycrystalline matrix by heating and quenching using either a laser or an electric pulse.[2,3] The information can be read by measuring the different reflectivities or resistivities of the two phases, and erased by using a pulse of different energy to recrystallize the material.[2] To further improve device characteristics such as transformation speed and resistance,[4] it is vital to understand, and to have full control over, the phase change mechanism between the crystalline and the amorphous phases. In order to understand the phase change mechanism, the structures of both the crystalline and the amorphous phases have to be characterized. In the case of $Ge_2Sb_2Te_5$ (GST), several structures have been proposed for both the crystalline and the amorphous phase, based on experimental data[5] and theoretical studies,[6,7] but so far no structure has been unambiguously identified as the correct one. An important question addressed here is whether the amorphous phase is a "frozen in" disorder[8] or a result of a thermally activated transformation ("flip") from one structure to another.[5] As we show, there are problems with the mechanisms so far proposed, and so in this paper we propose a mechanism based on density functional theory (DFT) and reverse Monte Carlo atomistic calculations and tested against the reduced density function (RDF) obtained from experimental diffraction data.

GST has both a cubic and a hexagonal crystalline phase.[8] The phase involved in the rapid switching is known to be cubic[9] and generally thought to be a distorted NaCl structure with Te on one sublattice and Ge, Sb, and vacancies on the other,[8] although a variation of this structure has been proposed recently, based on DFT calculations.[7] In this study, we consider only the NaCl structure, since there is at present no experimental verification of the other structure and no clear amorphization mechanism or structure of the amorphous phase outlined in Ref. 7.

II. MODEL STRUCTURES

Recently Kolobov *et al.*[5] studied the structures of both crystalline and amorphous GST. For the crystalline phase, they proposed that atoms around a vacancy can be described in terms of a planar ring of Te, Sb, and Ge atoms, with the vacancy causing relaxation of the Te atoms (which move away from the vacancy) and of the Ge and Sb atoms (which move towards the vacancy). This model (here referred to as the KB model) is designed to explain the considerable width of the distribution of Ge-Te and Sb-Te nearest neighbor distances revealed by extended x-ray absorption fine structure (EXAFS) analysis. However, we have carried out DFT calculations for a vacancy in an ideal (NaCl) lattice, and these show that the Ge and Sb atoms relax away from the vacancy and that the Te atoms move toward the vacancy [Figs. 1(a) and 1(b)], in disagreement with the KB model. In our calculations, the distance of the movement depends on the species of atoms surrounding the atoms immediately next to the vacancy, but a considerable variation in Ge-Te and Sb-Te nearest neighbor distances is found, consistent with the experimental data in Ref. 5 which Kolobov *et al.* were considering. Our predicted relaxations agree with the results of Welnic *et al.*[6] for $Ge_1Sb_2Te_4$, and this calls into question the KB model put forward for the crystalline to amorphous phase transition, as it was based on the weakening of the bonds in the crystal lattice caused by the changes in the nearest neighbor distances.

In the KB model for the amorphization, the Ge atoms switch rapidly from their sixfold coordination in the NaCl structure to a configuration where they are coordinated by four Te atoms [Figs. 2(a) and 2(c) to Figs. 2(b) and 2(d)]. The resulting structure is proposed as the building block of the amorphous phase. However, in addition to the four Te atoms, the Ge atom is at least initially (before any diffusion

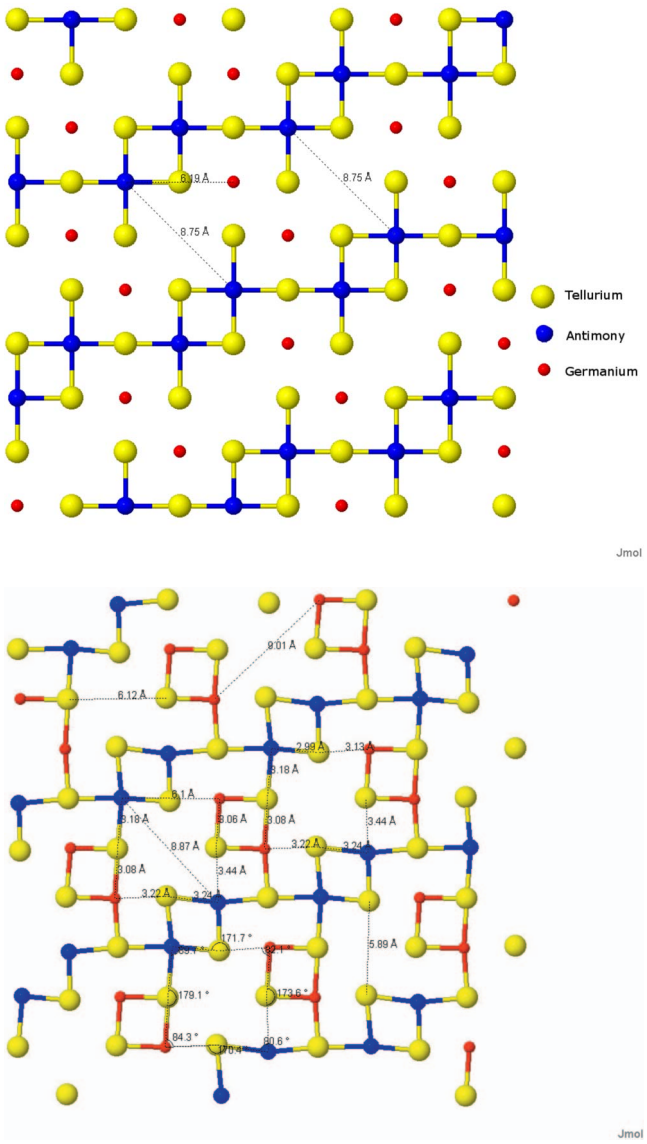

FIG. 1. (Color online) One layer of the crystalline phase of GST (a) before and (b) after relaxation. Ge atoms are shown in red (smallest), Te in yellow (largest), and Sb in blue. The arrangement of vacancies is as in Ref. 5. Angles and distances between atoms are given in the figures.

mediated changes occur) coordinated to three sites, each containing either a Sb or Ge atom or a vacancy. The "amorphization" according to the KB model is in effect a thermally activated switch from one structure to another. For such a switch to be feasible, there must be an energy barrier between the crystal and amorphous structures. To investigate whether such a barrier exists, we carried out DFT calculations for a Ge atom switching from a sixfold Te coordination (in the NaCl structure) to the configurations shown in Figs. 2(b) and 2(d). Bonds between either Ge and Ge or Ge and Sb are generally unfavorable in GST, although recent studies show that there may be a small number of Ge-Ge bonds.[10] However, since there are 20% vacancies on the same sublattice as Ge and Sb, some of the sites coordinating the flipped Ge atom may not be populated (i.e., may contain vacancies). For this reason, two possible configurations were considered

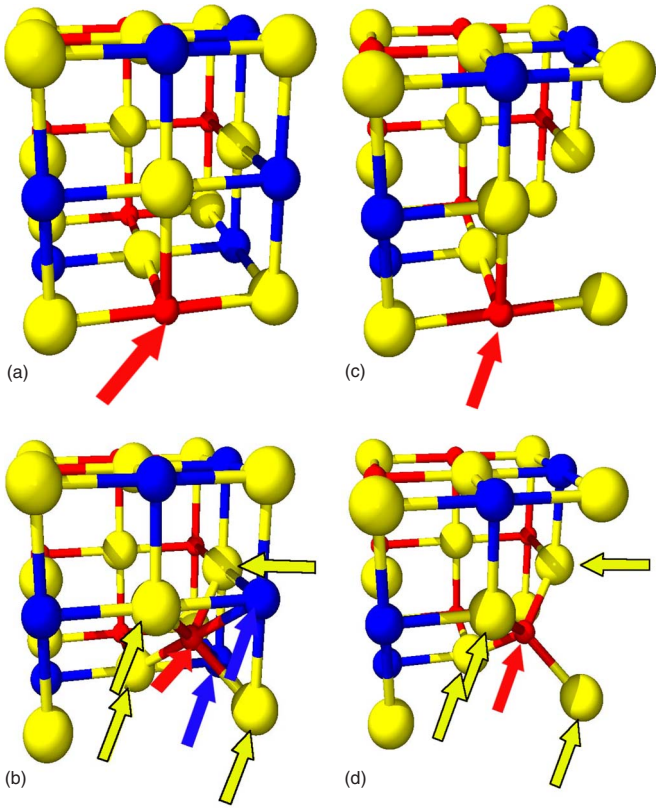

FIG. 2. (Color online) Atomic configurations before and after the flip. One unit cell of the atomic arrangement before and after the flip for [(a) and (b)] case 1 and [(c) and (d)] case 2 is shown. The red (short dark) arrows point at the Ge atom undergoing the flip. The yellow (long light with border) and blue (long light) arrows point at the Te and Sb nearest neighbor atoms, respectively, after the flip.

as shown in Fig. 2: In case (1), the Ge atom is coordinated to two Sb atoms in addition to the four Te atoms (i.e., one vacancy) [Figs. 2(a) and 2(b)], and in case (2), the Ge atom is coordinated to four Te atoms, without any coordination to Sb or Ge atoms (i.e., three vacancies) [Figs. 2(c) and 2(d)]. The existence of a barrier for switching between the configurations of Figs. 2(a) and 2(b), or between the configurations of Figs. 2(c) and 2(d), was investigated by calculating the energy of the system for the Ge atom being at various points between the configurations shown in Figs. 2(a) and 2(b) [the actual calculation cells (195 atoms) were larger than the ones shown in Fig. 2]. This was repeated for Figs. 2(c) and 2(d). It should be noted that the accurate calculation of a barrier height would require taking into account different atomic pathways from the initial to the final position. However, the existence of a barrier can be ruled out if there exists even one pathway without a barrier. Therefore, using our method, we can give an upper limit for the barrier height or rule out the existence of a barrier. The results in Fig. 3 show that while for the pathway we have chosen a barrier (i.e., a local maximum) exists for case (2) [i.e., there is a barrier between Figs. 2(c) and 2(d)], there is no barrier for case (1) [i.e., between Figs. 2(a) and 2(b)]. To check these predictions, the configurations of both Figs. 2(b) and 2(d) were allowed to relax to

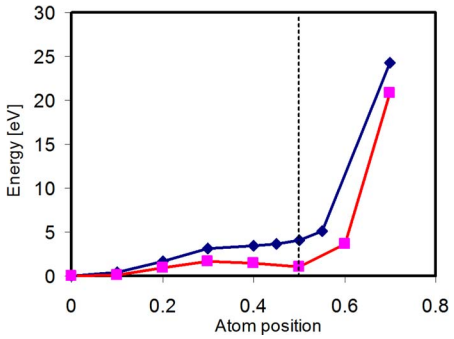

FIG. 3. (Color online) Energies for the transitions shown in Figs. 2(a)–2(d). The energy difference between a "perfect" NaCl lattice and a lattice with a Ge atom moving along the path from a sixfold to a fourfold Te coordination is shown. The blue (upper) line shows case (1) [Figs. 2(a) and 2(b)] and the red (lower) line case (2) [Figs. 2(c) and 2(d)]. The vertical dashed line shows the "equilibrium" position of the flipped atom [position of the flipped Ge atom in Figs. 2(b) and 2(d)].

determine equilibrium configurations. In case (1), Fig. 2(b) reverted to Fig. 2(a) (i.e., the Ge atom moved back to the NaCl crystalline position), as expected since we had shown that no energy barrier exists between the NaCl lattice and Fig. 2(b). For case (2), relaxation of Fig. 2(d) resulted in the Te atoms surrounding the Ge atom moving away from the Ge atom, so that the Ge-Te bond length was close to 3.0 Å [as opposed to 2.68 Å in Fig. 2(c)].

To study the situation further, DFT based molecular dynamics simulations were carried out for case (2), for a simulation time of 2 ps and for temperatures of 400 and 500 K. It was found that while the structure of Fig. 2(d) was stable at both temperatures for the investigated time scale, as expected from the local minimum in Fig. 3, the movement of the flipped Ge atom was significantly larger than that of the surrounding atoms, again as expected because of the shallowness of the local minimum.

If these results are interpreted in the context of the KB model, a transformation in that model is favorable only if there are no Sb atoms surrounding the site to which the Ge atom moves, i.e., if the flipped Ge is surrounded by four vacancies and four Te atoms as in Fig. 2(d). This is a very special, and rather unlikely, situation. Furthermore, the bonds between the Ge atom and the Te atoms would be rather weak in this case, which makes this an unlikely building block for the amorphous phase.

Because of these and similar shortcomings of the existing models, we propose a different building block for the amorphous phase as shown in Fig. 4(b). It is obtained by taking the eight atoms (two Sb, two Ge, and four Te atoms) in a plane around a vacancy in the crystalline phase of Fig. 1(a) and relaxing them, in the absence of any other atoms other than the eight, using DFT calculations. Figure 4(b) shows the resulting configuration. For reasons given below, we propose this distorted ring as the building block of the amorphous phase, with many similar rings embedded in an environment of other misaligned rings and additional Te atoms (to keep the correct stoichiometry), and distorted [Fig. 4(c)] by the local environment. (Of course, this choice of a planar ring of eight atoms around a particular vacancy is arbitrary, and could be any of the three {100} planes with the vacancy at the center. So we can envisage these rings on all three {100} planes.)

III. EXPERIMENTAL RDF STUDY

To test this model, we obtained electron diffraction patterns from amorphous GST thin films produced by magnetron sputtering and converted them into RDFs.[11] (We chose electron diffraction since data can be obtained from extremely small volumes which can be selected with high spatial accuracy,[12,13] which is not possible if one uses x-ray or neutron diffraction. While this capability was not crucial to the experiments in this work, it provides a basis for later work to be performed on real devices. Moreover, the quality of RDF data obtained from electron diffraction experiments is comparable with that from x-ray or neutron diffraction.[14])

Figure 4(a) shows the RDF obtained from electron diffraction from our amorphous GST thin film. The accuracy of our method is demonstrated by the fact that the first and second peak positions in our RDF agree well with the peak positions for the Ge-Te, Sb-Te, and Te-Te nearest neighbors measured by Kolobov *et al.* using EXAFS [Fig. 4(a)]. Additionally, our electron diffraction RDF shows some structure at higher distances which is not available from the EXAFS data. Figure 4(a) has the first peak in the amorphous GST at 2.7 Å as compared to 3.01 Å in an ideal NaCl-type crystalline structure (lattice constant $a=6.03$ Å). The second peak is close to that of crystalline GST, while the third peak of the crystalline structure disappears in the RDF of the amorphous material.

Interestingly, the interatomic distances between Ge-Te (2.67 Å) and Sb-Te (2.81 Å) in the ring of Fig. 4(b) are close to the peak positions of the RDF as well as to the Ge-Te and Sb-Te distances reported by Kolobov *et al.* in Ref. 5. Distortion of the rings would account for broadening of the peaks in the RDF. Misalignment of the rings with respect to each other also agrees with the fact that the third nearest neighbor peak of the crystalline phase all but disappears in the RDF of the amorphous phase, since the third nearest neighbor peak originates from out-of-plane interatomic distances which are not found in the planar ring structure. Consequently, an RDF of such an amorphous structure made up of (1) rings distorted along one axis and (2) additional Te atoms placed as a link between rings and by (3) adding a random misalignment between rings shows great similarity to the RDF measured from the amorphous structure [Fig. 2(a)]. It should be emphasized that this structure was created without any energetic considerations.

We therefore propose that these rings could form the building blocks of the amorphous structure, since the forces on the rings in a disordered environment may cancel out on average, leaving their shapes approximately intact. While this averaging is difficult to show using energetic calculations due to the model sizes that would be necessary, it is shown below that it is possible to assemble them into a structure with the same RDF as the experimentally measured RDF.

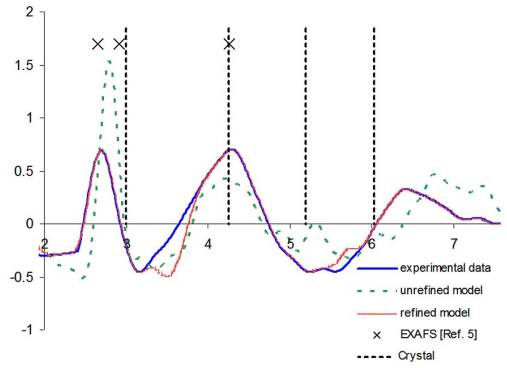

(a)

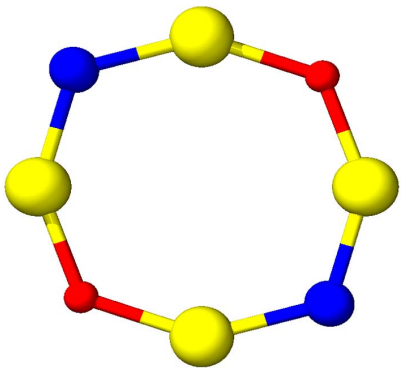

(b)

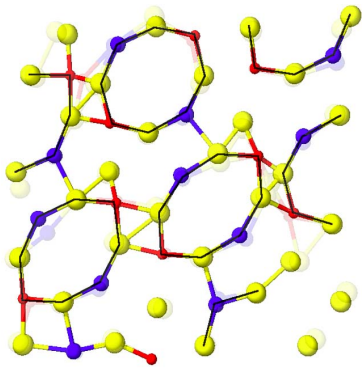

(c)

FIG. 4. (Color online) RDF and building blocks of the amorphous phase. (a) shows the RDF acquired experimentally from a GST thin film (black line) of the unrefined distorted ring model (dashed line) and of the model after reverse Monte Carlo refinement (dotted line). The positions of the Ge-Te, Sb-Te, and Te-Te nearest neighbor distances determined using EXAFS in Ref. 5 are shown (+), as well as the distances as they would be in a perfect NaCl-type crystal with $a=6.03$ Å (vertical, dashed lines). (b) shows the ring obtained after relaxing the atoms around a vacancy without any surrounding environment [Ge, red (smallest); Te, yellow (largest); Sb, blue] and (c) shows a layer of the distorted ring model before (strong colors) and after (weak colors) refinement.

IV. STRUCTURE REFINEMENT

This proposed structure was implemented in a model with 388 atoms and refined against the experimental electron diffraction RDF data using a reverse Monte Carlo (RMC) program similar to that developed by Keen and McGreevy.[15] The initial and final RDFs (after 500 000 refinement steps) are shown in Fig. 4(a). Figure 4(c) shows a part of both the unrefined and the refined structure. The distorted rings can still clearly be observed in the final, refined structure [Fig. 4(c)]. It was found that the atoms stayed relatively close to their original positions (average movement 0.47 Å) in 500 000 refinement steps despite the fact that no closest distance criterion was set in the RMC procedure, thereby enabling relatively free atom movement. The coordination numbers obtained from the refined structural model agree with Refs. 10 and 16 within the error of their measurement and are considerably below the fourfold coordination suggested by Kolobov *et al.* for the Ge coordination [the coordination numbers in the unrefined (refined) model are 3.62 (3.35) for Ge, 3.25 (3.01) for Sb, and 2.44 (2.36) for Te].

This proposed model has distorted planar rings as its building block. The phase transformation mechanism can be explained in terms of these rings as follows: On quenching, atoms (not having moved far from their original positions) assemble into rings to minimize the nearest neighbor energy. Since the structure of these rings is related to the original structure in the crystal of atoms around vacancies, the phase transformation from these rings to the crystalline state could be rapid.

This distorted ring structure could also provide an explanation of the influence of dopant atoms on the phase transformation. The introduction of low concentrations of dopant atoms may distort or misalign the rings, significantly influencing the transformation. The transformation speed and power efficiency in phase change materials have previously been demonstrated experimentally to be related to doping.[17,18] Further experimental work to elucidate the relationship between the atomic structure and doping is in progress.

V. METHODS

A. RDF from electron diffraction

The electron diffraction technique developed by Cockayne and McKenzie[11] for obtaining RDFs from thin films has been successfully applied to the determination of the structure in a range of different material systems.[11,14,19] The RDF is given by $\mathrm{RDF}(r)=4\pi r*[\rho(r)-\rho_0]$, where r is the distance from the atom in the origin, $\rho(r)$ the density at distance r, and ρ_0 the average density. Recent progress in both the experimental technique and instrumentation has extended the technique to give the RDF from small volumes (to 1 nm diameter) of amorphous materials[12,13] which can be selected with high accuracy. The imaging capabilities of a transmission electron microscope can be used to identify areas of interest, and areas on the sample with a diameter of down to 1 nm can be selected for analysis. The electron diffraction intensity $I(q)$ is collected to unusually (for electron diffrac-

tion) high scattering angles, from which the static structure factor $S(k)$ and $G(r)$ can be determined. We recognize at the outset that $G(r)$ is only the first order correlation function, which does not encompass medium or long range order. We also recognize that electron diffraction alone does not allow partial distribution functions to be extracted directly, which are only accessible through model refinement.

B. Reverse Monte Carlo

The RMC algorithm[15,20] is similar to the Metropolis Monte Carlo algorithm but instead of minimizing the energy of a given structure, the deviation between an experimental and a modeled dataset is minimized. It is widely used to recover atomistic arrangements from x-ray and neutron diffraction data[21,22] and has been used previously to recover the structure of amorphous carbon[23,24] and, with a slight variation of the method, the structure of C70 fullerenes[19] from electron diffraction data. Generally, the result of RMC calculations is not unique and therefore constraints have to be imposed on atomic movements and arrangements. The aim of this work was, however, to test the similarity between the atomic arrangement in the unrefined and the refined model. Therefore, no constraints were imposed on atom movement. In this work, the refinement was performed against an experimentally determined $G(r)$ between 2 and 7.5 Å.

C. DFT simulations

The total energy calculations performed in this paper have been performed by means of DFT within the generalized gradient approximation (GGA) using the package of linear combination of atomic-type orbitals (PLATO).[25] This code has recently undergone a major development to allow modeling of defects[26] in crystalline structures and *ab initio* molecular dynamics simulations of semiconductor amorphous alloys.[27] The calculations were performed using the relativistic pseudopotentials of Hartwigsen *et al.*[28] with the Perdew-Burke-Ernzerhof[29] GGA for the exchange and correlation functional. The code uses strictly localized atomlike basis functions. These are found by solving for an atom in an external spherical potential well $U(r)$, where the potential $U(r)$ is assumed to diverge for $r > r_c$ and r_c is a user-defined cutoff radius. This condition results in a set of basis functions vanishing at $r = r_c$ and retaining nonvanishing first and second derivatives at that point. To ensure that these derivatives vanish at r_c, the functions are multiplied by the factor $1 - \exp[-(r - r_c)^2/(2\sigma^2)]$, where σ is an adjustable parameter. This forms a very efficient basis set that is ideal for treating large systems within DFT simulations. All orbitals are cut off at the critical radius r_c, of 8.0 a.u., and their tails are smoothed over a distance σ of about 1.5 a.u. The present work uses a minimum optimized basis set for GST materials that is convenient for molecular dynamics simulations. In order to verify the validity of this basis set, *ab initio* calculations were also performed by the Vienna *ab initio* simulation package (VASP) using pseudopotentials with electron configurations of $4s^2 4p^2$ for Ge, $5s^2 5p^2$ for Sb, and $5s^2 5p^2$ for Te generalized by the projector augmented wave (PAW) approach.[30–32] All atoms were relaxed until the forces on them were less than 1 mRy/a.u. and the relaxation convergence for ions was 0.1 mRy.

VI. CONCLUSIONS

In conclusion, we have presented a different model for the rapid phase change GST material, based on the experimental data and *ab initio* calculations, which has significant advantages over previous models. In this model, the amorphous structure is based on distorted and misaligned rings. The misalignment is introduced by the heating during amorphization due to weak interring bonds. During the phase change, these rings essentially stay intact and deform due to the stronger intraring bonds. They act as the bridge between the crystalline and amorphous phases.

ACKNOWLEDGMENTS

D.N.M. is supported by EURATOM and United Kingdom EPSRC. C.L. is supported by the EPSRC and Linacre College, Oxford.

[1] T. Ohta and S. R. Ovshinsky, in *Photo-induced Metastability in Amorphous Semiconductors*, edited by A. V. Kolobov (Wiley-VCH, Berlin, 2003), p. 310.
[2] M. H. R. Lankhorst, B. W. Ketelaars, and S. M. Wolters, Nat. Mater. **4**, 347 (2005).
[3] H. F. Hamann, M. O'Boyle, Y. C. Martin, M. Rooks, and H. K. Wickramasinghe, Nat. Mater. **5**, 383 (2006).
[4] B. Liu, Z. Song, T. Zhang, J. Xia, S. Feng, and B. Chen, Thin Solid Films **478**, 49 (2005).
[5] A. V. Kolobov, P. Fons, A. I. Frenkel, A. L. Ankudinov, J. Tominaga, and T. Uruga, Nat. Mater. **3**, 703 (2004).
[6] W. Welnic, A. Pamungkas, R. Detemple, C. Steimer, S. Bluegel, and M. Wuttig, Nat. Mater. **5**, 56 (2006).
[7] Z. Sun, J. Zhou, and R. Ahuja, Phys. Rev. Lett. **96**, 055507 (2006).
[8] N. Yamada, MRS Bull. **21**, 48 (1996).
[9] N. Yamada, E. Ohno, K. Nishiuchi, N. Akahira, and M. Takao, J. Appl. Phys. **69**, 2849 (1991).
[10] D. A. Baker, M. A. Paesler, G. Lucovsky, S. C. Agarwal, and P. C. Taylor, Phys. Rev. Lett. **96**, 255501 (2006).
[11] D. J. H. Cockayne and D. R. McKenzie, Acta Crystallogr., Sect. A: Found. Crystallogr. **A44**, 870 (1988).
[12] W. McBride and D. J. H. Cockayne, J. Non-Cryst. Solids **318**, 233 (2003).
[13] W. McBride, D. J. H. Cockayne, and D. Nguyen-Manh, Ultramicroscopy **96**, 191 (2003).
[14] D. Ozkaya, W. McBride, and D. J. H. Cockayne, Interface Sci. **12**, 321 (2004).

[15] D. A. Keen and R. L. McGreevy, Nature (London) **344**, 423 (1990).
[16] B. Hyot, X. Biquard, and L. Poupinet, EPCOS Symposium (unpublished), http://www.epcos.org/pdf_2001/Hyot.pdf (2001).
[17] R. Kojima and Y. Noboru, Jpn. J. Appl. Phys., Part 1 **40**, 5930 (2001).
[18] H. Seo, T. H. Jeong, J. W. Park, C. Yeon, S. J. Kim, and S. Y. Kim, Jpn. J. Appl. Phys., Part 1 **39**, 745 (2000).
[19] D. R. McKenzie, D. A. Davis, D. J. H. Cockayne, D. A. Muller, and A. M. Vassallo, Nature (London) **355**, 622 (1992).
[20] R. L. McGreevy, J. Phys.: Condens. Matter **13**, R877 (2001).
[21] H. W. Sheng, W. K. F. Luo, M. Alamgir, J. M. Bai, and E. Ma, Nature (London) **436**, 419 (2006).
[22] M. G. Tucker, A. L. Goodwin, M. T. Dove, D. A. Keen, S. A. Wells, and J. S. O. Evans, Phys. Rev. Lett. **95**, 255501 (2005).
[23] D. G. McCulloch, D. R. McKenzie, C. M. Goringe, D. J. H. Cockayne, W. McBride, and D. C. Green, Acta Crystallogr., Sect. A: Found. Crystallogr. **A55**, 178 (1999).
[24] G. Opletal, T. C. Petersen, I. K. Snook, I. Yarovsky, and D. G. McCulloch, J. Phys.: Condens. Matter **17**, 2605 (2005).
[25] S. D. Kenny, A. P. Horsfield, and H. Fujitani, Phys. Rev. B **62**, 4899 (2000).
[26] D. Nguyen-Manh, A. P. Horsfield, and S. L. Dudarev, Phys. Rev. B **73**, 020101(R) (2006).
[27] K. Kohary, V. M. Burlakov, D. G. Pettifor, and D. Nguyen-Manh, Phys. Rev. B **71**, 184203 (2005).
[28] C. Hartwigsen, S. Goedecker, and J. Hutter, Phys. Rev. B **58**, 3641 (1998).
[29] J. P. Perdew, K. Burke, and M. Ernzerhof, Phys. Rev. Lett. **77**, 3865 (1996).
[30] G. Kresse and J. Hafner, Phys. Rev. B **47**, 558 (1993).
[31] G. Kresse and J. Furthmuller, Phys. Rev. B **54**, 11169 (1996).
[32] G. Kresse and J. Furthmuller, Comput. Mater. Sci. **6**, 15 (1996).